

Synthesis, characterization and hepatoprotective effect of silymarin phytosome nanoparticles on ethanol-induced hepatotoxicity in rats

Arezoo Gohari Mahmoudabad^{1,2*}, Fatemeh Gheybi^{3*}, Mohsen Mehrabi^{2*}, Alireza Masoudi⁴, Zeinab Mobasher⁵, Hamid Vahedi^{6,7}, Anneh Mohammad Gharravi⁸, Fatemeh Sadat Bitaraf⁹, Seyed Mahdi Rezaayat Sorkhabadi⁵

¹Student Research Committee, School of Medicine, Shahroud University of Medical Sciences, Shahroud, Iran

²Department of Medical Nanotechnology, School of Medicine, Shahroud University of Medical Sciences, Shahroud, Iran

³Department of Medical Biotechnology and Nanotechnology, Faculty of Medicine, Mashhad University of Medical Sciences, Mashhad, Iran

⁴Department of Pharmacology, School of Medicine, Shahroud University of Medical Sciences, Shahroud, Iran

⁵Department of Pharmacology, School of Medicine, Tehran University of Medical Sciences (TUMS), Tehran, Iran

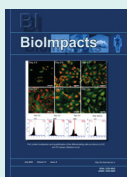
⁶Clinical Research Development Unit, Imam Hossein Hospital, Shahroud University of Medical Sciences, Shahroud, Iran

⁷Department of Gastroenterology, School of Medicine, Shahroud University of Medical Sciences, Shahroud, Iran

⁸Tissue Engineering and Stem Cell Research Center, Shahroud University of Medical Sciences, Shahroud, Iran

⁹Department of Medical Biotechnology, School of Medicine, Shahroud University of Medical Sciences, Shahroud, Iran

Article Info



Article Type:

Original Article

Article History:

Received: 13 Oct. 2021

Revised: 25 June 2022

Accepted: 13 Sep. 2022

ePublished: 30 May 2023

Keywords:

Silymarin

Phytosome

Nanoparticles

Alcoholic liver disease

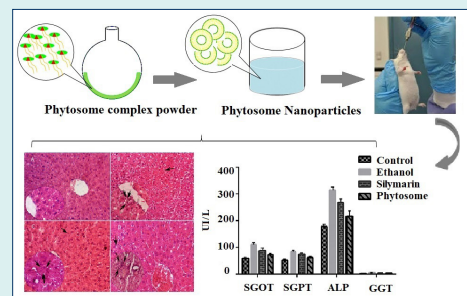
Abstract

Introduction: Silymarin proved to be a beneficial herbal medicine against many hepatic disorders such as alcoholic liver disease (ALD). However, its application is restricted due to its low bioavailability and consequently decreased efficacy. We herein used a nano-based approach known as “phytosome”, to improve silymarin bioavailability and increase its efficacy.

Methods: Phytosome nanoparticles (NPs) were synthesized using thin film hydration method. NPs size, electrical charge, morphology, stability, molecular interaction, entrapment efficiency (EE %) and loading capacity (LC %) were determined. Moreover, *in vitro* toxicity of NPs was investigated on mesenchymal stem cells (MSCs) viability using MTT assay. *In vivo* experiments were performed using 24 adult rats that were divided into four groups including control, ethanol (EtOH) treatment, silymarin/EtOH treatment and silymarin phytosome/EtOH, with 6 mice in each group. Experimental groups were given 40% EtOH, silymarin (50 mg/kg) and silymarin phytosome (200 mg/kg) through the gastric gavage once a day for 3 weeks. Biochemical parameters, containing ALP, ALT, AST, GGT, GPx and MDA were measured before and after experiment to investigate the protective effect of silymarin and its phytosomal form. And histopathological examination was done to evaluate pathological changes.

Results: Silymarin phytosome NPs with the mean size of 100 nm were produced and were well tolerated in cell culture. These NPs showed a considerable protective effect against ALD through inverting the biochemical parameters (ALP, ALT, AST, GGT, GPx) and histopathological alterations

Conclusion: Silymarin phytosomal NPs can be used as an efficient treatment for ALD.



Introduction

Alcoholic liver disease (ALD) is a global health issue with no effective therapeutic option. Although its pathological mechanisms are not fully understood despite previous investigations, oxidative stress and inflammation are

the main mechanisms involved in ALD pathogenesis.^{1,2} Therefore, therapeutic strategies have mainly focused on these pathological mechanisms.^{3,4}

Various studies have shown the effects of alcohol on oxidative damage and free radicals.⁵⁻⁷ During ethanol



*Corresponding author: Mohsen Mehrabi, Email: mehrabi@shmu.ac.ir



© 2023 The Author(s). This work is published by BioImpacts as an open access article distributed under the terms of the Creative Commons Attribution Non-Commercial License (<http://creativecommons.org/licenses/by-nc/4.0/>). Non-commercial uses of the work are permitted, provided the original work is properly cited.

metabolism, hydroxyethyl radicals produced by the microsomal mono oxygenase system stimulate lipid peroxidation; also, through immunological processes and the hepatic proteins CYP2E1, they induce the production of specific antibodies that can cause oxidative stress and finally, liver damage.⁶⁻⁹ It has been shown that ethanol can induce liver damage in animal models, which can be assessed by measuring liver enzymes: alkaline phosphatase (ALP), alanine transaminase (ALT), aspartate transaminase (AST) and gamma-glutamyl transferase (GGT), as well as measuring antioxidant enzymes: glutathione peroxidase (GPx) and lipid peroxidation index: Malondialdehyde (MDA), and conducting histological investigation. In the case of oxidative stress, the amount of liver enzymes (ALT, AST, ALP and GGT) and peroxidative index (MDA), and the damage to liver cells are increased, while the amount of antioxidant enzyme (GPx) in serum is decreased.^{10,11}

Currently, there are limited numbers of synthetic drugs against ALD, including bicyclol, tiopronin and bifendate, providing short-term symptomatic improvement. Therefore, there is a dire need for new therapeutic strategies to cope with this devastating disease. During the last decade, an increasing number of studies have been conducted to discover the healing properties of natural compounds against ALD; of these, silymarin has been proved to be a desirable agent due to its antioxidant and anti-inflammatory attributes. Silymarin is a flavonoid extracted from the milk thistle *Silybum marianum*, which shows a large range of therapeutic properties such as anti-inflammatory, anti-cancer, anti-allergy, anti-thrombosis and anti-fibrotic properties, as well as anti-lipid peroxidation.^{12,13} This substance has been used to treat fatty liver, mushroom poisoning, alcohol abuse, etc.¹⁴⁻¹⁶ However, in spite of the strong antioxidant and anti-inflammatory features of silymarin, as observed in the previous *in vitro* experiments, it showed minimal beneficial effect against ALD in the *in vivo* condition, which could be mainly due to its low bioavailability.¹⁷ There are four main reasons for the low bioavailability of this substance; these include increased phase II metabolism, low permeability in intestinal epithelial cells, skimp solubility in water, and the fast excretion of urine and bile.¹⁸ Therefore, developing strategies for increasing silymarin bioavailability has gained a great deal of attention among researchers; among these strategies, nano-based carriers have been shown to be an efficient approach to enhance drug bioavailability, decrease drug use, mitigate drug adverse effects and reduce drug waste.¹⁹ In this regard, the phytosomal form of silymarin has been proved to be a desirable strategy to increase silymarin bioavailability.^{20, 21} Phytosomal form of silymarin is a combination of silymarin and phosphatidylcholine, which is prepared by solvent evaporation and converted to phytosomal vesicles by thin film hydration; this exhibits higher solubility, better absorption, better membrane permeability and a more stable chemical composition,

thus leading to a better bioavailability drug system for silymarin.²²⁻²⁵ Phytosomal form of silymarin has been previously produced; its physical properties, such as including size, surface charge, loading capacity (LC), entrapment efficiency (EE), particle morphology and stability, were evaluated; however, its therapeutic effect against ALD has not been reported. Therefore, we herein performed this research to produce the phytosomal form of silymarin, examine its physical properties and investigate its therapeutic potentials against ALD in a rat model of ALD.

Materials and Methods

Chemicals and reagents

All the chemicals and cell culture medium components were purchased from Sigma Aldrich (Sigma-Aldrich, Steinheim, Germany).

Methods

Preparation of silymarin–phosphatidylcholine complex (SPC)

Silymarin/SLM (S0292) and soybean phosphatidylcholine/SPC (Lecithin p3644) were mixed based on a ratio of 1/2.5 (according to their molecular weight; 1 g of silymarin and 4 g of phosphatidylcholine) and then dissolved in 100 ml acetone ($\geq 99.5\%$) on the thermal stirrer (1000 rpm - 25°C) overnight. Then the sample was put in a rotary evaporator for 1 hour (speed 180 rpm - 50°C) to remove the solvent and then moved into the freeze dryer for 24 hours to entirely remove the solvent remainder. The prepared SPCs were moved into a plastic bag and stored under -20°C for the next step.²⁶⁻²⁸

Determination of silymarin content in the complex

Ten milliliters of the phytosomal solution was put in a centrifuge at 15000 for 1 hour, and the supernatant was carefully removed using a micropipette and dissolved in methanol to destroy phytosomal vesicles. Then necessary dilution was done and the amount of silymarin was measured by applying UV Spectrophotometer at 288 nm and subsequently, the Beer-Lambert law. Finally, the trapping efficiency and loading capacity were calculated by the appendix equations, as shown below²⁷:

$$\%EE = \frac{\text{amount of silymarin loaded}}{\text{total amount of silymarin}} \times 100$$

$$\%LC = \frac{\text{amount of silymarin loaded}}{\text{total lipid content}} \times 100$$

Fourier transformed infrared (FTIR) spectroscopy

Molecular interactions between the components of the compound were investigated using the infrared scanning of pure silymarin, phosphatidylcholine and silymarin phytosome via FTIR (Rayleigh, China). Briefly, each sample (~2 mg) was uniformly blended with potassium bromide (KBR, ~200 mg) and pressed under a pressure of 10 Ton/nm² to catch circular transparent discs. Each

analysis had 45 scans, with a resolution of 4 cm^{-1} in the wavelength range 4000 to 400 cm^{-1} . Obtained results were analyzed by the resolution FTIR control software connected to the instrument.

Preparation of silymarin phytosome-nanoparticles (SPCs-NPs)

Silymarin phytosome-nanoparticles were prepared through the hydration method. Briefly, the SPCs complex was dispersed in 50 ml distilled water with agitation on a thermal stirrer (20 minutes - 15 000 rpm - 50°C); then it was vibrated for 4 minutes using a probe sonicator with a 60% amplifier, based on 5 second on-off intervals. At this stage, the size, zeta potential, PDI, morphology and molecular interaction of phytosome NPs were examined, and the collected phytosome-nanosuspensions were stored at -60°C for 24 hours by adding 1% w/v Trehalose as the freeze-drying cryoprotectant agent. After the adequate pre-freeze process, the samples were lyophilized by using a freeze dryer for 48 hours at -57°C . The acquired solid powders were kept at -20°C for characterization studies.²⁶⁻²⁸

Particle size, polydispersity index (PDI), zeta potential and morphology analyses

Dynamic light scattering (DLS, HORIBA, SZ-100) was used to obtain the particle size and zeta potential of SPCs-NPs. The morphology of the dried SPCs-NPs was evaluated using a Field Emission Scanning Electron Microscopy (FESEM; Zeiss, Sigma 300-HV, Germany), as follows: samples were covered with gold in a Fine Coat Ion Sputter. Analysis was done on the covered sample by putting up a pinch of the sample in the field emission scanning electron microscope; then surface morphology was observed and photographed.

SPCs-NPs stability analysis

The stability of SPCs-NPs optimized and coated with Trehalose cryoprotectant was evaluated using the freeze-thaw method. Samples were placed in three cycles of freeze-thaw operation with the lowest temperature of -80°C and the highest temperature of 4°C . After each cycle, some characteristics including morphology, vesicle size, vesicle size distribution, zeta potential and phytosome structure were evaluated to specify the stability of SPCs-NPs.^{26,28-30}

Release study

The amounts of silymarin release were determined using cellulose dialysis bags containing phytosome suspension in phosphate buffered saline (PBS) and simulated intestinal fluids (SIF) media. The dialysis tubes were hanged in two 100 mL beakers that contained 50 mL of PBS and the SIF media (pH = 7.4). Then the solutions were stirred at 100 rpm in a thermal incubator shaker at $37 \pm 0.5^{\circ}\text{C}$; the 2 mL samples were collected at definite time intervals, and equivalent volumes of fresh PBS and SIF media were added. All samples were filtered, diluted by methanol and analyzed by UV spectrophotometer at 288 nm; the percentages of leaked silymarin were determined using its calibration curve.^{31,32}

In vitro assay

Cell culture

Human mesenchymal stem cells (MSCs) were purchased from Pasteur Institute, Tehran, Iran. The cells were grown in a complete DMEM supplemented with 1% antibiotic-antimycotic solution and 10% heat-inactivated FBS. Cells were retained in T25 flasks at 37°C in a moistened incubator containing 5% CO_2 and all experiments were performed in 96-well plates.

MTT test

MSC cells were cultured for 24 hours in the defined medium. MSC cells were treated with different doses of silymarin in the range of $15.625\text{ }\mu\text{g/mL}$ - $1000\text{ }\mu\text{g/mL}$; also, its phytosomes was in the range of $31.25\text{ }\mu\text{g/mL}$ - $4000\text{ }\mu\text{g/mL}$ during 48 and 72 hours. The media were removed after 48 and 72 hours, and $100\text{ }\mu\text{L}$ of the 1 mg/mL solution of MTT was added for 4 hours; then $100\text{ }\mu\text{L}$ of the pure DMSO was added to each well, and their absorbance was measured at 570 nm by the Plate Reader. The optical density (OD) was proportional to the blue product (formazan) formed by MTT and the activity of living cell succinate dehydrogenase.

In vivo assay

Twenty-four male Wistar rats ($200 \pm 20\text{ g}$) were obtained from the Experimental Center of Shahroud University of Medical Sciences (Shahroud, Iran) and kept at $22 \pm 2^{\circ}\text{C}$, with $5\% \pm 5$ humidity, and a 12-hour light-dark period with free access to water and food for a week before the experiment. The animals were divided randomly into four groups (n=6) including (1) normal control group (no damage), (2) alcohol group (40% EtOH, orally), (3) alcohol + silymarin (50 mg/kg), (4) alcohol + silymarin phytosome (200 mg/kg).

Two hours before alcohol consumption, the phytosome suspension of silymarin and silymarin was given to the treated mice (3 and 4) by gastric gavage for 21 days.³³ 24 hours after the last treatment, the rats were anesthetized by intraperitoneal injection of $75\text{-}100\text{ mg/kg}$ 10% ketamine and 10 mg/kg xylazine 2%. Blood samples were then taken quickly and clotted. Serums were obtained by centrifugation at 3000 rpm for 8 minutes at 4°C and placed in a very low-temperature freezer until AST, ALT, ALP, GGT, GPx and MDA were assayed. Therefore, the liver was isolated, removed from the blood with ice-cold salt, and immediately refrigerated until Mason and H&E trichrome staining was assayed.

Biochemical assay

Plasma levels of ALT, AST, ALP, GGT, GPx and MDA were measured using the assay kits, according to the corresponding protocols.

Histopathological studies

The liver tissue was fixed with 10% formalin at normal temperature; after 1 day, it was placed in paraffin. The tissues were cut into $5\text{ }\mu\text{m}$ -thick slices and stained with

H&E and Masson's trichrome. Pathological samples were assessed under a light microscope.

Statistical analysis

Statistical analysis and comparison of the groups were done via one-way analysis of variance (ANOVA) and *t* test using GraphPad Prism 9 software; *P* values less than 0.05 were considered significant; also, all diagrams were prepared in GraphPad Prism 9 software.

Results

Characterization of silymarin phytosome nanoparticles

Particle size, PDI, zeta potential and morphology

Optimized size, zeta potential and PDI of SPCs-NPs were 105.16 ± 7.303 nm (mean \pm SD, *n*=10), -10.681 ± 1.6 mV (mean \pm SD, *n*=10), and 0.374 ± 0.07 (mean \pm SD, *n*=10), respectively (Table 1). Zeta potential is an acute factor to evaluate the consistency of the nanosuspension system. We found that the zeta potential of SPCs-NPs had enough charge to inhibit aggregation. These results illustrated that the SPCs-NPs were almost homogeneous and constant. The NPs morphology showed an average size smaller than that obtained through DLS, which could be due to the hydrodynamic diameter of the NPs (Fig. 1).

Molecular interactions

FTIR spectroscopy was used to consider the probable molecular interactions between silymarin and phosphatidylcholine in the solid state. Infrared spectra of silymarin, phosphatidylcholine, the physical mixture of

Table 1. Size, zeta potential and PDI of SPCs-NPs

Number	Size (nm)	Zeta Potential (mV)	PDI
1	105.6	-10.3	0.359
2	104.7	-9.5	0.402
3	95.6	-9.8	0.354
4	97.2	-10.2	0.318
5	97.5	-10.9	0.411
6	110.7	-8.9	0.427
7	109	-15.01	0.346
8	119	-11.5	0.402
9	99.8	-10.6	0.501
10	112.5	-10.1	0.221
SD	7.30358816	1.597575976	0.07058959

silymarin and phosphatidylcholine, and SPCs are shown in Fig. 2. There were no new peaks in the SPCs sample when compared to the physical mixture. However, a small change in the tensile vibration peaks of $-P = O$ (1284 cm^{-1}) and $-C = O$ (1730 cm^{-1}) was observed in phospholipid molecules in the SPCs spectrum. The new tensile vibration peaks $-P = O$ and $-C = O$ in SPCs were 1292 cm^{-1} and 1739 cm^{-1} , respectively. This showed that there were interactions between silymarin and phosphatidylcholine. In addition, the free tensile vibration peak of $-O-H$ (3448 cm^{-1}) silymarin in the SPCs spectrum was expanded and displaced, thus indicating the formation of a hydrogen

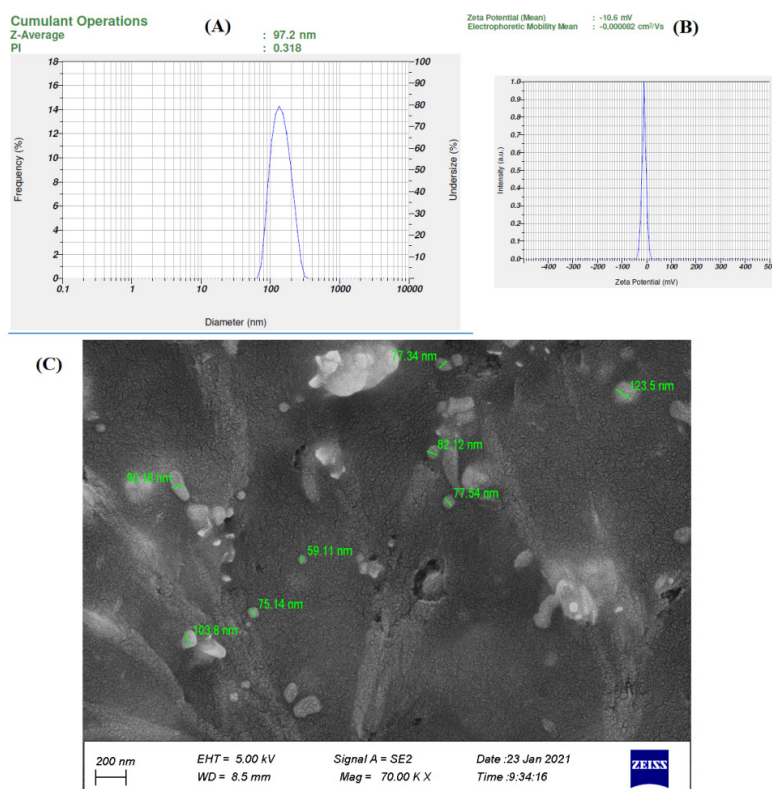


Fig. 1. Characteristics of SPCs-NPs. Size, PDI (A) and zeta potential (B) were measured by DLS. Morphology of NPs (C) as shown by FESEM.

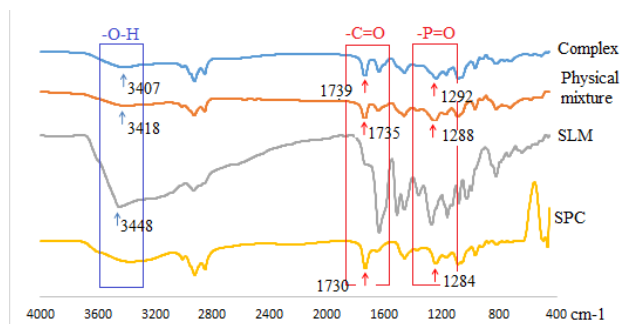


Fig. 2. FTIR spectra of soybean phosphatidylcholine (SPC), silymarin (SLM), physical mixture, and complex (SPCs).

bond between free -O-H in silymarin and -P = O in phospholipids. We, therefore, concluded that no new conjugated bonds were formed between silymarin and phosphatidylcholine and that hydrogen bonding was a weak intermolecular interaction between the hydroxyl silymarin groups and carbonyl group, and the phosphoryl phosphatidylcholine group.

Entrapment efficiency and loading capacity

The results of the UV spectrophotometer and the subsequent application of Beer-Lambert's law showed that 1.92 mg of silymarin was in a 10 mg batch (containing 8 mg of phosphatidylcholine and 2 mg of silymarin). Thus, the entrapment efficiency and loading capacity were obtained at 96% and 24%, respectively.

Release study

The release of silymarin from the phytosomal complex into the PBS over 240 minutes was about 83%, as shown in Fig. 3; in the intestinal medium, this was about 20%, which was much higher in the PBS than in the SIF. This difference could be related to the intermolecular bonds between silymarin and lipids and intestinal secretions.

Stability of NPs

A stability test was accomplished on an optimized formulation with a concentration of 5% SPCs-NPs based on a ratio of 1: 2.5 silymarin/phosphatidylcholine and 1% w/v trehalose cryoprotectant. SPCs-NPs were constant according to the tendency for fusion, massification and vesicle infraction over the three cycles of the freeze-thaw stability test. Size, PDI and zeta potential of vesicles after the freeze-thaw test for 3 cycles, respectively, were increased from 100.1 nm to 105.6 nm, 0.313 to 0.359 and -33.4 mV to -35.0 mV; these changes were not, however, significant. Also, the FTIR spectra of the samples and NPs morphology were similar before and after the test. All of these results, therefore, indicated the physical stability of the composed NPs (Fig. 4).

In vivo results

Effects of silymarin/silymarin phytosome on the levels of ALT, ALP, AST, GGT, GPx enzymes and MDA oxidative index in the experimental groups

The levels of ALP, ALT, AST, GGT and MDA oxidative

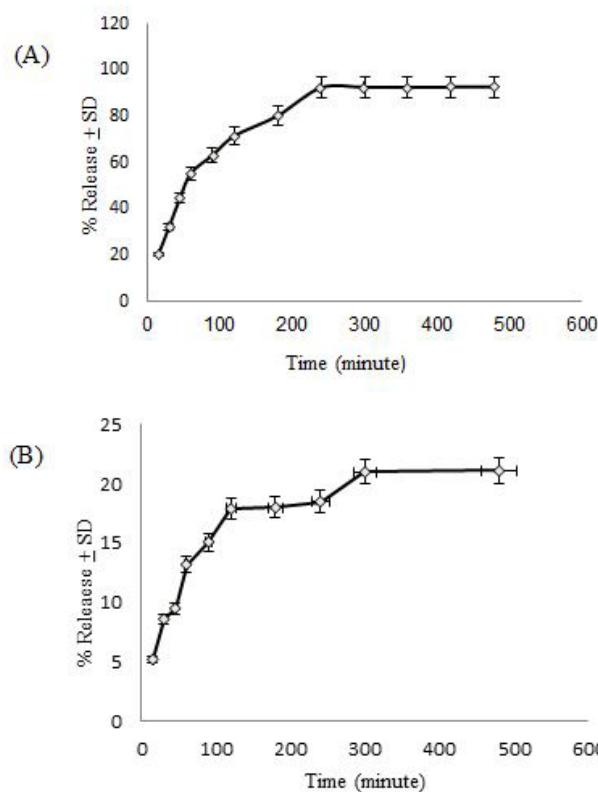


Fig. 3. Release of silymarin from phytosomal complex to PBS (A) and SIF (B) at different time points.

index in the alcohol group were increased significantly, as compared to the control group ($P < 0.001$); meanwhile, the levels of these factors were decreased significantly in the phytosome of silymarin and silymarin groups; these changes were more notable in the silymarin phytosome group ($P < 0.05$). Also, the level of GPx was significantly decreased in the ethanol group when compared to the control group ($P < 0.001$), and it was increased in the silymarin and silymarin phytosome groups; however, it was more elevated in the silymarin phytosome group, when compared to the silymarin group ($p < 0.05$), as shown in Fig. 5.

Histopathology test results

Hematoxylin and Eosin (H&E): Microscopic evaluation of liver tissues (Fig. 6 (I)) in the control group showed that the liver lobules had a clear structure with hepatic cords arranged around the central veins (A). However, in the ethanol group, liver H&E staining showed the abnormal lobular structure of the liver, irregular liver rope structure, and apparent interstitial infiltration of inflammatory cells (arrows) (B). Compared with the silymarin group (C), phytosome could significantly reduce the penetration of ethanol-induced inflammatory cells and hepatic cord (arrows) disorder (D).

Masson's trichrome

As shown in Fig. 6 (II), collagen fibers were stained in several biopsy specimens from the ethanol group; however, few collagenous fibers were found in the

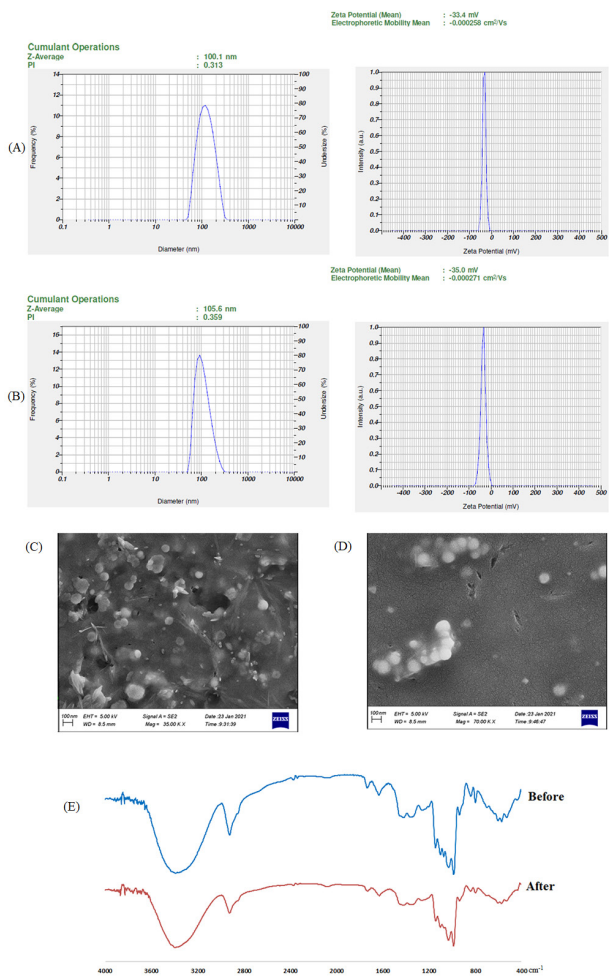


Fig. 4. The influence of the freeze-thawing test on the SPCs-NPs; (A) Particle size, PDI, and zeta potential before the Freeze-Thawing test; (B) Particle size, PDI, zeta potential after the Freeze-Thawing test; (C) Morphology before Freeze-Thawing test; (D) Morphology after Freeze-Thawing test; (E) FTIR spectra before and after the freeze-thawing test.

silymarin group (1C) and the phytosome group (1D). Moreover, the control group tissue exhibited a normal portal triad cellular architecture that consisted of the portal venule, arteriole and bile duct (1A). Micrographs in the area of the portal triad showed the normal collagen fiber deposition; collagen fibers were stained very light blue (arrows) around the boundary of the portal triad (2A), and the phytosome group illustrated the area of PT (2D), which was similar to the control group. The ethanol and silymarin group exhibited collagen fiber deposition, which was increased at the area of the portal triad (2B, 2C). The micrograph in the area of the portal triad also illustrated the abundance of collagen fiber deposition. In addition, collagenous fibers were stained in the boundary of the central vein of several biopsy specimens of the ethanol group (3B); however, few collagenous fibers were found around the boundary of the central vein of silymarin and phytosome groups (3C, 3D).

In vitro results

Due to the lack of access to healthy human liver cells,

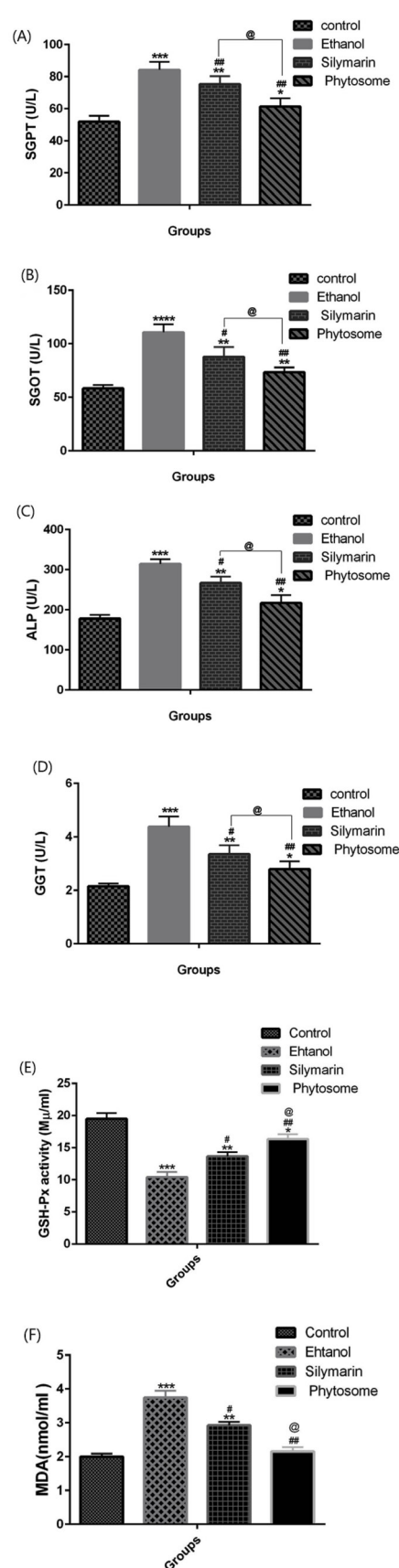


Fig. 5. Effects of silymarin and silymarin phytosome on plasma levels of ALT, AST, ALP, GGT, GPx and MDA in rat model of alcohol-induced liver damage; Data are presented as means ± SEM (n=6 per group); *P < 0.05, **P < 0.01 & ***P < 0.001 versus the control group; #P < 0.05 & ##P < 0.01 versus alcohol group; @P < 0.05 versus silymarin group.

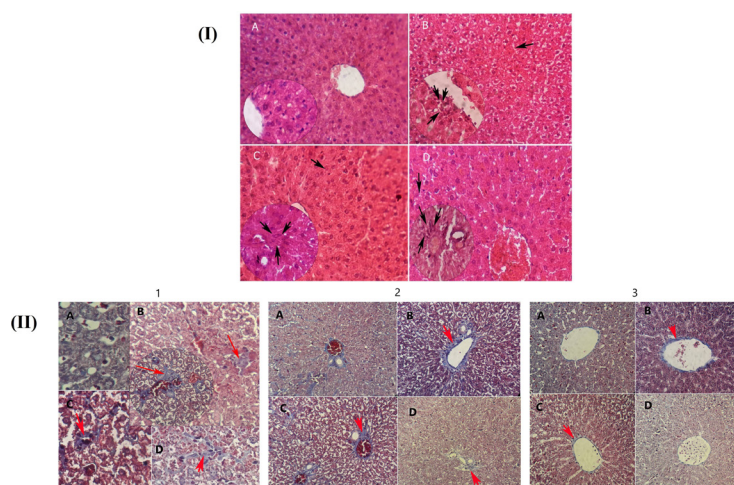


Fig. 6. (I) Effects of silymarin and silymarin phytosome on histopathological changes in alcohol-induced liver injury in rats; (A) Control group; (B) Ethanol group; (C) Silymarin group; (D) Silymarin phytosome group. Liver sections were stained with H&E X400; Arrows indicate inflammatory cells, abnormal hepatic lobular structure and disorderly liver cord structure. (II) Histopathological examination; 1. Photomicrographs of liver tissue; 2. Photomicrographs of the portal triad of liver tissue; 3. photomicrographs of the central vein of liver tissue; (A) Control group; (B) Ethanol group; (C) Silymarin group; (D) Silymarin phytosome group (magnification: $\times 40$).

we used MSCs instead. These stem cells have the ability to differentiate into various types of cells in the body, including liver cells, making them a potentially better alternative.

MTT test results showed that after 48 and 72 hours of exposure to silymarin and silymarin phytosome, MSC cells were increased in low concentrations; however, at the concentration of 125 $\mu\text{g}/\text{mL}$ silymarin and 250 $\mu\text{g}/\text{mL}$ silymarin phytosome, the number of cells was decreased significantly. Further reduction was observed at higher concentrations, and the lowest number of cells was obtained at 1000 $\mu\text{g}/\text{mL}$ silymarin and 4000 $\mu\text{g}/\text{mL}$ silymarin phytosome. Overall, these results showed the lower toxicity of silymarin phytosome, as compared to silymarin; also, the results indicated that toxicity of both agents was dose but not time-dependent (Fig. 7).

Discussion

In this study, we investigated the hepatoprotective effects

of silymarin and silymarin phytosome on ethanol-induced hepatotoxicity in a male ALD rat model. Biochemical and histopathological analyses showed the adverse effects of ethanol on the liver cell culture and liver of the ALD rat model, which was significantly reversed in both silymarin and silymarin phytosome treated groups, as compared to control group animals; however, silymarin phytosome showed higher improvement when compared to silymarin.

Histopathological findings of this study showed that both silymarin and silymarin phytosomes significantly reduced ethanol-induced inflammatory cell penetration and hepatic umbilical cord disorder. Also, the administration of silymarin and phytosome silymarin improved oxidative stress and liver enzyme activity; however, these beneficial effects were more significant in the phytosome silymarin-treated group than in the silymarin one. In addition, the survival rate of hepatocytes in the phytosome silymarin group was higher than that in the silymarin one.

According to our results, previous studies have shown

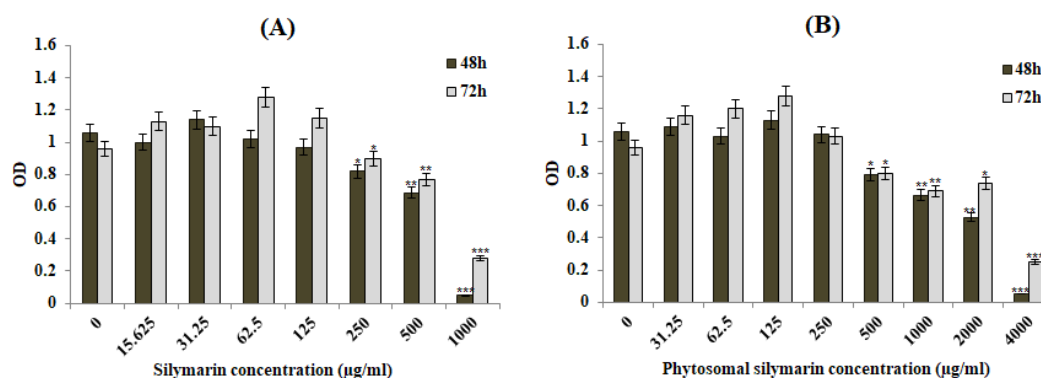


Fig. 7. Viability changes in MSCs treated with (A) silymarin; and (B) silymarin phytosome; OD value of control cells (unexposed cells) was taken as 100% viability (0% cytotoxicity) in 48 hours and 72 hours. Data were reported as mean \pm SD. * $P < 0.05$, ** $P < 0.01$ & *** $P < 0.001$ versus the control group.

the adverse effects of ethanol on the liver, as well as the therapeutic effects of silymarin against ethanol poisoning in mice and rat models with ALD.²⁶ A proposed mechanism for the pathogenesis of ALD is through the activation of Kupffer cells (KCs) and resident liver macrophages.^{34,35} KCs are activated by intestinal endotoxin/lipopolysaccharide (LPS) and other stresses induce factors like reactive oxygen species (ROS), tumor necrosis factor α (TNF- α), interleukins, and chemical traction agents for neutrophils. They release cytotoxic agents that disrupt the function and viability of the nearby cells.³⁶ Chronic exposure to ethanol increases intestinal permeability and causes intestinal endotoxin/LPS to penetrate the liver and activate KCs. Activated KCs produce large amounts of ROS, chemokines and proinflammatory cytokines, which can lead to the infiltration of other inflammatory cells and ultimately, liver damage.³⁷ Chronic exposure to ethanol can also increase the level of TNF- α cell surface receptors, resulting in the formation of oxidative stress-related pro-inflammatory compounds like MAA (MDA reacts with proteins and acetaldehyde to form additional protein compounds).³⁸ Furthermore, it has been suggested that cytochrome P4502E1 (CYP2E1), the main source of ROS in ALD,³⁸ is expressed in KCs and the small intestine; its activation by ethanol increases intestinal permeability and elevate LPS-induced TNF- α production by KCs.³⁹ The suggested mechanism underpinning the therapeutic effects of Silymarin in ALD patients is targeting ROS, TNF- α and LPS,^{40,41} as depicted in Fig. 8.

Protective effects of silymarin on the liver have also been reported in clinical trials. Saller and colleagues, for example, indicated that silymarin significantly reduced fatality in patients with liver cirrhosis.⁴² In another study, Mirnezami et al showed, in a randomized clinical trial, that silymarin could be used as an effective, low-complication, and low-cost treatment to solve the problem of the elevated liver enzymes ALT and AST following isotretinoin.⁴³ Numerous studies have also

demonstrated the antioxidant, anti-apoptotic and hepatic protective properties of silymarin. Silymarin (especially silybin or silybinin) has been shown to be a very powerful antioxidant and free radical scavenger.⁴⁴⁻⁴⁷

Our results, thus, showed that these beneficial effects could be increased through phytosomal formulation. Previous studies have also indicated that phosphatidylcholine in the phytosome not only carries biologically active flavonoids, but also acts as a biologically active nutrient for liver disease, including alcoholic hepatic steatosis^{48,49}; moreover, plant extracts in phytosomes are protected against degradation by gastrointestinal secretions and intestinal bacteria due to their lipid-resistant bond.⁵⁰ In this regard, serum analysis of 23 healthy individuals that used silybin-phosphatidylcholine (silybinin is the primary active flavonolignan in silymarin extract) or silymarin showed the higher bioavailability of silybin-phosphatidylcholine when compared to silymarin.^{51,52} These results were also observed in animals; also, the oral administration of phytosome complexes (containing phosphatidylcholine and silybin) showed higher bioavailability, as compared to silymarin, in dogs.⁵³ Although our study provided the first evidence on the protective effects of the phytosomal form of silymarin against ALD, Kumar et al. had previously shown an increase in the protective properties of silymarin following liposomal formulation. Their results showed higher cell viability, improved liver function, and antioxidant and anti-inflammatory effects of liposomal silymarin, as compared to bulk silymarin, in the in vitro and in vivo models of alcohol-induced hepatotoxicity.⁵⁴ The effect of silymarin on MSCs had previously been investigated by Ahmadi-Ashtiani et al. They showed that silymarin increased MSC proliferation by day 7 at two different concentrations (50 L and 100 L) and then decreased cell proliferation by raising the exposure time. This finding confirms our results, showing that silymarin initially increased MSC proliferation, which was then decreased over time.⁵⁵

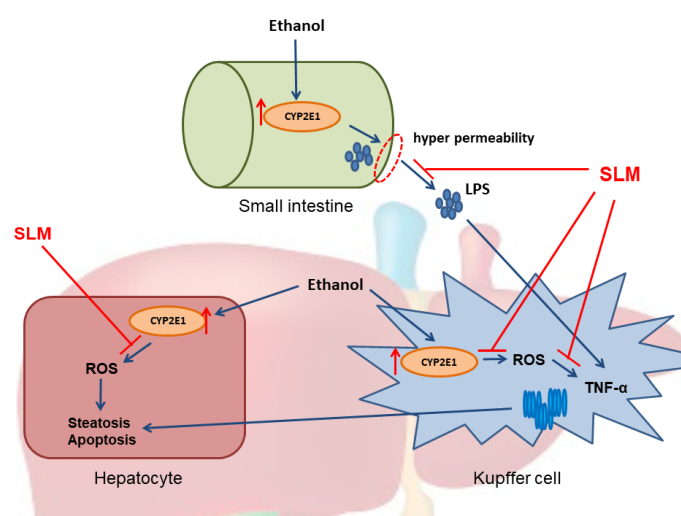


Fig. 8. The pathogenesis mechanisms of ethanol on the liver and the protective role of silymarin.

Research Highlights

What is the current knowledge?

- ✓ Silymarin is a hepatoprotective compound.
- ✓ Phytosome can enhance the bioavailability of silymarin, therefore, enhancing its therapeutic properties

What is new here?

- ✓ Silymarin phytosome NPs proved to be an efficient treatment option for alcoholic liver disease, and also showed lower toxicity compared to a bulk form of silymarin due to a lower amount of incorporated silymarin in its phytosomal form

Overall, our results showed that phytosomes containing silymarin could increase the antioxidant properties of silymarin and ameliorate hepatic oxidative stress more effectively. Therefore, it can be used as a therapeutic option against ALD.

Conclusion

To conclude, in the present study, stable silymarin phytosome NPs with an average size of 100 nm were synthesized. These phytosomes showed higher beneficial effects against ALD, when compared to bulk silymarin, through reducing oxidative stress, inflammation, and lipid peroxidation, which led to improved liver function in the rat model of ALD. Further studies are, however, needed to evaluate the clinical efficacy of this formulation against ALD and other liver disorders.

Authors' contribution

Conceptualization: Mohsen Mehrabi, Fatemeh Gheybi.

Methodology: Mohsen Mehrabi, Fatemeh Gheybi, Alireza Masoudi.

Validation: Arezoo Gohari Mahmoudabad, Fatemeh Sadat Bitaraf.

Formal analysis: Arezoo Gohari Mahmoudabad, Zeinab Mobasher.

Investigation: Arezoo Gohari Mahmoudabad.

Resources: Mohsen Mehrabi, Fatemeh Gheybi.

Data curation: Arezoo Gohari Mahmoudabad, Alireza Masoudi.

Visualization: Arezoo Gohari Mahmoudabad.

Supervision: Mohsen Mehrabi, Fatemeh Gheybi.

Project administration: Mohsen Mehrabi, Seyed Mahdi Rezaayat Sorkhabadi.

Funding acquisition: Mohsen Mehrabi.

Writing—original draft preparation: Arezoo Gohari Mahmoudabad.

Writing—review and editing: Zeinab Mobasher, Anneh Mohammad Gharravi, Hamid Vahedi.

Competing Interests

The authors declare no conflict of interest.

Ethical Statement

This experiment was performed according to the instructions of the National Institute of Health for the care and use of laboratory animals and approved by the Committee for the Care and Use of Institutional Animals at Shahrood University of Medical Sciences (IR.SHMU. REC.1398.122). This study was approved by the Ethics Committee of Shahrood University of Medical Sciences, Shahrood, Iran (IR. SHMU. REC.1398.122).

Funding

The present study was supported by Shahrood University of medical sciences as an MSc Thesis. We hereby acknowledge the research deputy for Grant No. 9871.

References

1. Seitz HK, Bataller R, Cortez-Pinto H, Gao B, Gual A, Lackner C, et al. Alcoholic liver disease. *Nat Rev Dis Primers* 2018; 4: 1-22. <https://doi.org/10.1038/s41572-018-0021-8>
2. Lamas-Paz A, Hao F, Nelson LJ, Vázquez MT, Canals S, Del Moral MG, et al. Alcoholic liver disease: Utility of animal models. *World J Gastroenterol.* 2018; 24: 5063. <https://doi.org/10.3748/wjg.v24.i45.5063>
3. Bellentani S. The epidemiology of non-alcoholic fatty liver disease. *Liver Int* 2017; 37: 81-4. <https://doi.org/10.3748/wjg.v24.i45.5063>
4. Walsh K, Alexander G. Alcoholic liver disease. *Postgrad Med J* 2000; 76: 280-6. <https://doi.org/10.1136/pmj.76.895.280>
5. Teschke R. Alcoholic liver disease: alcohol metabolism, cascade of molecular mechanisms, cellular targets, and clinical aspects. *Biomedicines* 2018; 6: 106. <https://doi.org/10.3390/biomedicines6040106>
6. Jiang Y, Zhang T, Kusumanchi P, Han S, Yang Z, Liangpunsakul S. Alcohol metabolizing enzymes, microsomal ethanol oxidizing system, cytochrome P450 2E1, catalase, and aldehyde dehydrogenase in alcohol-associated liver disease. *Biomedicines* 2020; 8: 50. <https://doi.org/10.3390/biomedicines8030050>
7. Dupont I, Lucas D, Clot P, Ménez C, Albano E. Cytochrome P4502E1 inducibility and hydroxyethyl radical formation among alcoholics. *J. Hepatol* 1998; 28: 564-71. [https://doi.org/10.1016/S0168-8278\(98\)80279-1](https://doi.org/10.1016/S0168-8278(98)80279-1)
8. Cho YE, Mezey E, Hardwick JP, Salem Jr N, Clemens DL, Song BJ. Increased ethanol-inducible cytochrome P450-2E1 and cytochrome P450 isoforms in exosomes of alcohol-exposed rodents and patients with alcoholism through oxidative and endoplasmic reticulum stress. *Hepatol. Commun* 2017; 1: 675-90. <https://doi.org/10.1002/hep4.1066>
9. Ullah U, Badshah H, Malik Z, Uddin Z, Alam M, Sarwar S, et al. Hepatoprotective effects of melatonin and celecoxib against ethanol-induced hepatotoxicity in rats. *Immunopharmacol. Immunotoxicol* 2020; 42: 255-63. <https://doi.org/10.1080/08923973.2020.1746802>
10. Elnaggar AS, El-Said EA, Ali R. Physiological and immunological responses of ducks (*Cairina moschata domestica*) to silymarin supplementation. *Egypt Poultry Sci J* 2021;40:895-913. <https://doi.org/10.21608/epsj.2021.177227>
11. El Rabey HA, Rezk SM, Sakran MI, Mohammed GM, Bahattab O, Balgoon MJ, et al. Green coffee methanolic extract and silymarin protect against CCL4-induced hepatotoxicity in albino male rats. *BMC Complement Med Ther* 2021; 21: 1-11. <https://doi.org/10.1186/s12906-020-03186-x>
12. Zalat Z, Kohaf N, Alm El-Din M, Elewa H, Abdel-Latif MMM. Silymarin: A promising cardioprotective agent. *Azhar Int J Pharm Med Sci* 2021; 1: 13-21. <https://doi.org/10.21608/aijpm.2021.52962.1014>
13. Sandhu N, Au J. Herbal Medicines for the Treatment of Nonalcoholic Steatohepatitis. *Curr Hepatol Rep* 2021; 20: 1-11. <https://doi.org/10.1007/s11901-020-00558-2>
14. Gillesen A, Schmidt HH-J. Silymarin as supportive treatment in liver diseases: A narrative review. *Adv Ther* 2020; 37: 1279-301. <https://doi.org/10.1007/s12325-020-01251-y>
15. Mengesha T, Sekaran NG, Mehare T. Hepatoprotective effect of silymarin on fructose induced nonalcoholic fatty liver disease in male albino Wistar rats. *BMC Complement Med Ther* 2021; 21: 1-13. <https://doi.org/10.1186/s12906-021-03275-5>
16. Hashem A, Shastri Y, Al Otaibi M, Buchel E, Saleh H, Ahmad R, et al. Expert Opinion on the Management of Non-Alcoholic Fatty Liver Disease (NAFLD) in the Middle East with a Focus on the Use of Silymarin. *Gastroenterol Insights* 2021; 12: 155-65. <https://doi.org/10.1007/s12325-020-01251-y>

- doi.org/10.3390/gastroent12020014
17. Marceddu R, Dinolfo L, Carrubba A, Sarno M, Di Miceli G. Milk Thistle (*Silybum marianum* L.) as a Novel Multipurpose Crop for Agriculture in Marginal Environments: A Review. *Agronomy* 2022; 12: 729. <https://doi.org/10.3390/agronomy12030729>
 18. Theodosiou E, Purchartová K, Stamatis H, Kolisis F, Křen V. Bioavailability of silymarin flavonolignans: drug formulations and biotransformation. *Phytochem Rev* 2014; 13: 1-18. <https://doi.org/10.1007/s11101-013-9285-5>
 19. Xie Y, Zhang D, Zhang J, Yuan J. Metabolism, transport and drug–drug interactions of silymarin. *Molecules* 2019; 24: 3693. <https://doi.org/10.3390/molecules24203693>
 20. Deng M, Chen H, Xie L, Liu K, Zhang X, Li X. Tea saponins as natural emulsifiers and cryoprotectants to prepare silymarin nanoemulsion. *LWT-Food Sci Technol* 2022; 156: 113042. <https://doi.org/10.1016/j.lwt.2021.113042>
 21. Di Costanzo A, Angelico R. Formulation strategies for enhancing the bioavailability of silymarin: the state of the art. *Molecules* 2019; 24: 2155. <https://doi.org/10.3390/molecules24112155>
 22. Vaishnavi A, Arvapalli S, Rishika P, Jabeen S, Karunakar B, Sharma J. A Review on Phytosomes: Promising Approach for Drug Delivery of Herbal Phytochemicals. *J Pharm Innov* 2021. <https://doi.org/10.35629/7781-0601289296>
 23. Zhu H-J, Brinda BJ, Chavin KD, Bernstein HJ, Patrick KS, Markowitz JS. An assessment of pharmacokinetics and antioxidant activity of free silymarin flavonolignans in healthy volunteers: a dose escalation study. *Drug Metab Dispos* 2013; 41: 1679-85. <https://doi.org/10.1124/dmd.113.052423>
 24. Sallam N, Sanad R, KHAFAGY E-S, Ahmed M, Ghourab M, Gad S. Colloidal delivery of drugs: present strategies and conditions. *Rec Pharma Biomed Sci* 2021; 5: 40-51. <https://doi.org/10.21608/rpbs.2020.30372.1070>
 25. Nanavati B. Phytosome: a novel approach to enhance the bioavailability of phytoconstituent. *Asian J Pharm* 2017; 11. <https://doi.org/10.22377/ajp.v11i103.1445>
 26. Chi C, Zhang C, Liu Y, Nie H, Zhou J, Ding Y. Phytosome-nanosuspensions for silybin-phospholipid complex with increased bioavailability and hepatoprotection efficacy. *Eur J Pharm Sci* 2020; 144: 105212. <https://doi.org/10.1016/j.ejps.2020.105212>
 27. Maryana W, Rahma A, Mudhakir D, Rachmawati H, editors. Phytosome containing silymarin for oral administration: Formulation and physical evaluation. *J Biomim Biomater Biomed Eng* 2015: Trans Tech Publ. <https://doi.org/10.4028/www.scientific.net/JBBBE.25.54>
 28. Maryana W, Rachmawati H, Mudhakir D. Formation of phytosome containing silymarin using thin layer-hydration technique aimed for oral delivery. *Mater Today Proc* 2016; 3: 855-66. <https://doi.org/10.1016/j.matpr.2016.02.019>
 29. Hua Z-Z, Li B-G, Liu Z-J, Sun D-W. Freeze-drying of liposomes with cryoprotectants and its effect on retention rate of encapsulated florafur and vitamin A. *Drying Technol* 2003; 21: 1491-505. <https://doi.org/10.1081/DRT-120024489>
 30. Samad A, Devarajan PV. Freeze thaw: a simple approach for prediction of optimal cryoprotectant for freeze drying. *AAPS PharmSciTech* 2010; 11: 304-13. <https://doi.org/10.1208/s12249-010-9382-3>
 31. El-Batal AI, Elmenshawi SF, Ali AMA, Goodha E. Preparation and characterization of silymarin nanocrystals and phytosomes with investigation of their stability using gamma irradiation. *Indian J Pharm Educ Res* 2018; 52: S174-S83. <https://doi.org/10.5530/ijper.52.4s.96>
 32. Molaveisi M, Shahidi-Noghabi M, Naji-Tabasi S. Vitamin D3-loaded nanophytosomes for enrichment purposes: Formulation, structure optimization, and controlled release. *J Food Process Eng* 2020; 43: e13560. <https://doi.org/10.1111/jfpe.13560>
 33. Joseph S, Abdul Vahab A, Harindran J, Iyer RS. Evaluation of hepatoprotective activity of polyherbal (HEPIN) against alcohol induced hepatotoxicity in Wistar albino rats. *World J Pharm Res* 2018; 7: 146-155. <https://doi.org/10.20959/wjpr201817-13195>
 34. Dixon L, Barnes M, Tang H, Pritchard M, Nagy L. Kupffer cells in the liver. *Compr Physiol* 2013; 3: 785-97. <https://doi.org/10.1002/cphy.c120026>
 35. Smith K. Kupffer cells regulate the progression of ALD and NAFLD. *Nat Rev Gastroenterol Hepatol* 2013; 10: 503-13. <https://doi.org/10.1038/nrgastro.2013.140>
 36. Saberi B, Dadabhai AS, Jang Y-Y, Gurakar A, Mezey E. Current management of alcoholic hepatitis and future therapies. *J Clin Transl Hepatol* 2016; 4: 113-22. <https://doi.org/10.14218/JCTH.2016.00006>
 37. Parlesak A, Schäfer C, Schütz T, Bode JC, Bode C. Increased intestinal permeability to macromolecules and endotoxemia in patients with chronic alcohol abuse in different stages of alcohol-induced liver disease. *J Hepatol* 2000; 32: 742-7. [https://doi.org/10.1016/S0168-8278\(00\)80242-1](https://doi.org/10.1016/S0168-8278(00)80242-1)
 38. Zeng T, Zhang C-L, Xiao M, Yang R, Xie K-Q. Critical roles of Kupffer cells in the pathogenesis of alcoholic liver disease: from basic science to clinical trials. *Front Immunol* 2016; 7: 538. <https://doi.org/10.3389/fimmu.2016.00538>
 39. Yang L, Wu D, Wang X, Cederbaum AI. Cytochrome P4502E1, oxidative stress, JNK, and autophagy in acute alcohol-induced fatty liver. *Free Radic Biol Med* 2012; 53: 1170-80. <https://doi.org/10.1016/j.freeradbiomed.2012.06.029>
 40. Feng R, Chen J-H, Liu C-H, Xia F-B, Xiao Z, Zhang X, et al. A combination of Pueraria lobata and Silybum marianum protects against alcoholic liver disease in mice. *Phytomedicine* 2019; 58: 152824. <https://doi.org/10.1016/j.phymed.2019.152824>
 41. Federico A, Dallio M, Loguerco C. Silymarin/silybin and chronic liver disease: a marriage of many years. *Molecules* 2017; 22: 191. <https://doi.org/10.3390/molecules22020191>
 42. Saller R, Meier R, Brignoli R. The use of silymarin in the treatment of liver diseases. *Drugs* 2001; 61: 2035-63. <https://doi.org/10.2165/00003495-200161140-00003>
 43. Mirnezami M, Jafarimanesh H, Rezagholizamenjany M, Alimoradian A, Ranjbaran M. The effect of silymarin on liver enzymes in patients taking isotretinoin: A randomized clinical trial. *Dermatol Ther* 2020; 33: e13236. <https://doi.org/10.1111/dth.13236>
 44. Khazaei R, Seidavi A, Bouyeh M. A review on the mechanisms of the effect of silymarin in milk thistle (*Silybum marianum*) on some laboratory animals. *J Vet Med* 2022; 8: 289-301. <https://doi.org/10.1002/vms3.641>
 45. Ezhilarasan D, Lakshmi T. A Molecular Insight into the Role of Antioxidants in Nonalcoholic Fatty Liver Diseases. *Oxid Med Cell Longev* 2022; 2022. <https://doi.org/10.1155/2022/9233650>
 46. Aghemo A, Alekseeva OP, Angelico F, Bakulin IG, Bakulina NV, Bordin D, et al. Role of silymarin as antioxidant in clinical management of chronic liver diseases: a narrative review. *Ann Med* 2022; 54: 1548-60. <https://doi.org/10.1080/07853890.2022.2069854>
 47. Adelina J-AM. Clinical studies of silymarin as a protective agent against liver damage caused by anti-TB drugs, methotrexate, and in cases of chronic hepatitis C and diabetes mellitus. *Pharmacogn J* 2022; 14. <https://doi.org/10.5530/pj.2022.14.46>
 48. Mahmoudabad GA, Shirshahi V, Mehrabi M, Gheybi F, Gharravi MA, Salehi M, et al. Phytosome: an effective transdermal drug delivery system for phytoconstituents. *Lett Drug Des Discov* 2022; 19: 1-. <https://doi.org/10.2174/1570180819666220615092854>
 49. Bharati R, Badola A. Phytosomes—a modernised and new technology: revolutionary progress in the field of pharmacy for enhanced bioavailability of cosmeceuticals and nutraceuticals. *World J Pharm Res* 2021. <https://doi.org/10.20959/wjpr202110-21164>
 50. Marczylo TH, Verschoyle RD, Cooke DN, Morazzoni P, Steward WP, Gescher AJ. Comparison of systemic availability of curcumin with that of curcumin formulated with phosphatidylcholine. *Cancer Chemother Pharmacol* 2007; 60: 171-7. <https://doi.org/10.1007/s00280-006-0355-x>

51. Méndez-Sánchez N, Dibildox-Martinez M, Sosa-Noguera J, Sánchez-Medal R, Flores-Murrieta FJ. Superior silybin bioavailability of silybin–phosphatidylcholine complex in oily-medium soft-gel capsules versus conventional silymarin tablets in healthy volunteers. *BMC Pharmacol Toxicol* 2019; 20: 1-6. <https://doi.org/10.1186/s40360-018-0280-8>
52. Pal P, Dave V, Paliwal S, Sharma M, Potdar MB, Tyagi A. Phytosomes—nanoarchitectures' promising clinical applications and therapeutics. *Nanopharm Adv Deliv Syst* 2021; 187-216. <https://doi.org/10.1002/9781119711698.ch9>
53. Filburn C, Kettenacker R, Griffin D. Bioavailability of a silybin–phosphatidylcholine complex in dogs. *J Vet Pharmacol Ther* 2007; 30: 132-8. <https://doi.org/10.1111/j.1365-2885.2007.00834.x>
54. Kumar N, Rai A, Reddy ND, Shenoy RR, Mudgal J, Bansal P, et al. Improved in vitro and in vivo hepatoprotective effects of liposomal silymarin in alcohol-induced hepatotoxicity in Wistar rats. *Pharmacol Rep* 2019; 71: 703-12. <https://doi.org/10.1016/j.pharep.2019.03.013>
55. Ahmadi-Ashtiani H, Allameh A, Rastegar H, Soleimani M, Barkhordari E. Inhibition of cyclooxygenase-2 and inducible nitric oxide synthase by silymarin in proliferating mesenchymal stem cells: comparison with glutathione modifiers. *J Nat Med* 2012; 66: 85-94. <https://doi.org/10.1007/s11418-011-0554-6>